Water Supply

Water Supply Vol 22 No 10, 7821 doi: 10.2166/ws.2022.237

Numerical simulation of pollution transport and hydrodynamic characteristics through the river confluence using FLOW 3D

Jafar Chabokpour [a,*] and Hazi Md Azamathulla[b]

[a] Hydraulic structures, civil engineering department, University of Maragheh, Maragheh, Iran
[b] Civil and Environmental Engineering, University of the West Indies, St. Augustine, Trinidad
*Corresponding author. E-mail: J.chabokpour@maragheh.ac.ir

JC, 0000-0002-6268-4415

ABSTRACT

The current study tried to investigate the hydrodynamic characteristics and the pollution mixing and dispersion from the sub-branch through the river confluence using the numerical model of Flow3D. A numerical model was used with length, width, and height of ($7 \times 1 \times 1$) m. Also, the nested mesh was used in the junction to refine the modeling and result depiction. It was observed that if there is a water level difference on both sides of the junction, the mixing will occur much faster, and only longitudinal mixing will prevail downstream of the junction. Therefore, it was concluded that to reduce the contamination effect through the river networks, the water level in the main channel should be higher than the sub-branch. In the flow separation zone, several clockwise vortices were observed, which become weaker by moving towards the outer wall of the channel. Also, the most significant velocity vectors and also the highest contaminant concentration was observed in this region. Moreover, the vertical distribution of pollution concentration showed that the contaminant concentration would be higher at large distances above the channel bed. The highest values of turbulent intensity and turbulent kinetic energy were also observed in flow recirculation zone. It was concluded that by increase of concentration gradient through the shear layers, the required mixing length for complete transverse pollution mixing would be decreased.

Key words: contaminant mixing, flow pattern, numerical simulation, river junction

HIGHLIGHTS

- To reduce the contamination effect through the river networks, the water level in the main channel should be higher than the sub-branch.
- In the flow separation zone of junction, several clockwise vortices were observed, which become weaker by moving towards the outer wall of the channel.
- The highest values of turbulent intensity and turbulent kinetic energy were also observed in flow recirculation zone.

INTRODUCTION

River junctions are the essential parts of a surface water network that play a crucial role in the sedimentary material motion and sedimentation and also the bedforms formation. Intense turbulence at junctions significantly affects the morphology of the substrate and mixing of contaminants (Chabokpour *et al.* 2020a). A river junction is a geomorphological point created at the intersection of two tributaries or a tributary to the mainstream and has a three-dimensional flow structure. Usually, the branch that is longer with more discharge is known as the main channel, and the ratio of the main channel discharge upstream of the confluence to the sub-branch discharge is known as the discharge ratio, and also the width ratio upstream of the junction is known as the width ratio. In general, the created river junctions are classified into two asymmetrical forms and Y shapes. There are many differences in hydrodynamics and other characteristics of these two types of confluences, leading to different studies in this area (Ghostine *et al.* 2013; Konsoer & Rhoads 2014; Yuan *et al.* 2018). Research on asymmetrical confluences is mostly based on the intersection angle and the ratio of the width of the two branches. Best (1988) concluded that the tributaries' intersection angle and discharge ratio significantly affect in-depth changes created through the river junctions.

In addition, a lot of researchers have been done on the bed differences between the two branches of the junction. Researchers have shown that this difference causes the mixing layer to shift and increase turbulence intensity (Best & Roy 1991; Biron *et al.* 1996a, 1996b).

Due to the creation of rotational currents through the stream confluences, several researchers have also studied the three-dimensional hydrodynamics of the junction using acoustic Doppler velocity meters. Weber *et al.* (2001) conducted a similar study in this field and analyzed the generated velocity vectors of turbulence kinetic energy. Furthermore, a similar experimental study at a 90-degree junction showed that the discharge ratio and the created flow pattern affect the vertical distribution of the average flow velocity. Yuan *et al.* (2016) observed that a stronger spiral current is formed and motion much further downstream at the junction by increasing the branch discharge. Moreover, in a coherent study, it was observed that the pressure gradient on the sides of the junction is the most critical factor influencing the flow structure, and the convective acceleration has a more negligible effect on the formed secondary currents (Song *et al.* 2012). Symmetrical confluences known as Y-shaped junctions have been studied. By researching this domain, several flow zones were identified through the stream junction (Liu *et al.* 2019). However, the overall observed current downstream of the junction is the spiral flow pattern and increasing the discharge ratio and the bed level difference make the spiral flow weaker. Rhoads & Sukhodolov (2001) suggested that spiral motion can enhance the mixing process through the junctions. In general, it can be said that six separate regions can be observed at the river junction that differ in terms of flow pattern. (I) Stagnation zone where the velocity decreases but never approaches zero; (II) flow deflection zone, where the flow is diverted to the outer wall; (III) flow separation zone, next to the downstream junction corner; (IV) maximum velocity zone, the distance between the shear layers downstream of the junction; (V) flow recovery zone, where the flow pattern returns to the normal conditions of the main channel and the drastic changes in the intersection area is decreasing; (VI) shear layers that are created under the influence of the robust velocity gradient between the main channel's separation zone and deflection zone (Best 1987) (Figure 1).

Previously most attempts have been made to calculate the flow depth and energy dissipation through the confluences. Also, it was tried to present some relationships in this area. Furthermore, calculating the dimensions and expansion of the separation zone has been one of the crucial goals of these studies (Webber & Greated 1966; Ramamurthy *et al.* 1988). Best & Reid (1984), using the vertical dye visualization through the junction showed that increasing the discharge ratio and confluence angle increases the width and length of the separation zone. Biron *et al.* (1996a, 1996b) examined the effect of bed level difference between the two sides of the junction on the dimensions and appearance of different typical zones created through the confluences. Sediment transport through the river confluence causes hydrodynamic changes and morphological variation of the stream. Also, the gradation of sediment particles introduced from different branches to the river junction causes variations in the dimensions of the downstream channel as well as the type and migration of bedforms (Mosley 1976; Richards 1980; Ashmore 1991; Bridge 1993; Ashmore & Gardner 2008; Best & Rhoads 2008). In many cases, created sedimentary processes

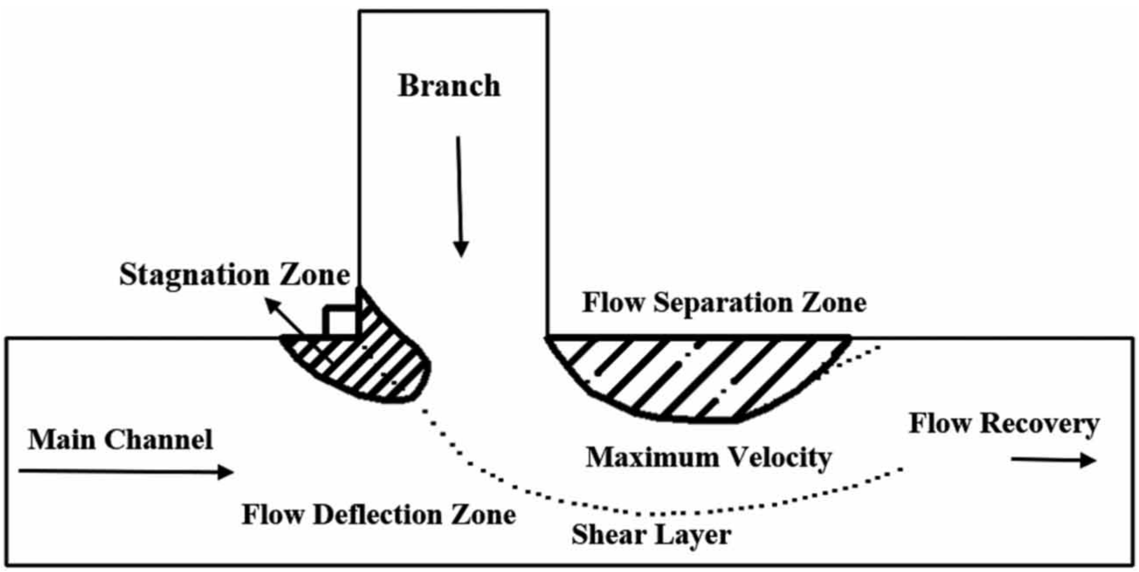

Figure 1 | Conceptual model of different flow pattern zones through the river confluence.

in the junctions cause land use and downstream flood management changes (Ettema 2008). In other words, it is sometimes said that these points are the main points for the river's biodiversity (Benda *et al.* 2004). Even at junctions that seem stable, hydraulic conditions are sometimes quite complex, further complicating contaminant motion path and dispersion (Biron & Lane 2008). It can be said that the scouring of the junction and the material transport are determined by the hydrodynamic conditions of inlet currents from the upstream branches and the downstream reach. Therefore, it can be explained that differing confluence hydraulic conditions may produce a variety of distinct sedimentology zones from sandy bar development to mud-filled scours (Best & Rhoads 2008). Moreover, understanding the confluence mobility plane and thus the potential spatial scouring surfaces is crucial to interpreting alluvial stratigraphy (Best & Ashworth 1997; Fielding & Gupta 2008). Several previous researchers have worked on the migration of scouring points through the junctions and have posed fundamental questions in this regard. Holbrook & Bhattacharya (2012) studied whether confluences can migrate enough to produce a scouring sufficiently resembling a cut valley. However, in the field studies, the confluence migration has been observed at a rate of several kilometers per year (Best & Ashworth 1997). Additionally, sharp angle junctions have been observed to change their plan over decadal timescales (Riley 2013). Ettema (2008) has studied bank erosion and bar bedform generation under the influence of floods events. On the other hand, Best (1988) and (Best & Roy 1991) have examined the bar migration due to the discharge ratio variation. Besides, some studies have been done on morphological variations and junction location due to sedimentation through the confluence zone. On a small scale, Shit & Maiti (2013) examined up- and downstream motion in the gully system due to the sediment load of branches. There is a broader theoretical basis for assuming the confluence position, and its morphology may develop significantly over time. Mosley (1976) proved the dynamic morphology of confluence. It is concluded that mostly confluences respond to upstream boundary conditions and each branch's sediment supply. It was mentioned that the junctions would be adjusted to three factors. Firstly, the upstream discharge condition and the momentum ratio of the interconnected branches. In other words, it is the momentum ratio between the branches that affect erosion or sedimentation as well as contaminant convection and dispersion (Mosley 1976; Best 1986, 1988; Best & Rhoads 2008). Even evidence and observations show that changes in bedforms affect the momentum ratio through the river junction (Boyer *et al.* 2006). This can happen under the influence of tributaries with different upstream climatic conditions or different seasonal conditions. Secondly, this can be influenced by the junction angle that controls the morphology of the scour as well as the morphology of the inlet branches (Mosley 1976; Best 1988; Sambrook Smith *et al.* 2005). It has also been observed that the junction angle in meandering channels changes over time with the meandering extension or cutoff.

Accurate water quality modeling through the streams is one of the most critical challenges for hydraulic engineers due to diverse human consumption (Chabokpour & Samadi 2020). Due to the complexity of the flow structure of river junctions, the interpretation of the pollutant mixing process is possible only with the help of the three-dimensional flow structure through the river junction (Chabokpour *et al.* 2020b). Previous researchers have been shown that the difference in bed level on both sides causes faster contaminant mixing (Biron *et al.* 2004; Schindfessel *et al.* 2015; Tang *et al.* 2018). The pollution mixing through the river confluences affects the contaminant concentration downstream of the junction (Chabokpour *et al.* 2020a). The operated turbulence models such as the Navier-Stokes and Reynolds models showed that the shear layer and the rotational flows are the most critical parameters in this mixing process (Tang *et al.* 2018). One of the basic features of river confluences is creating a mixture between inlet flows due to differences in flowing water characteristics such as temperature, suspended sediment concentration, contaminant concentration, etc. (Rhoads & Sukhodolov 2008). Previous studies such as Rhoads & Kenworthy (1998) and Ramón *et al.* (2013) observed that these differences in the water properties of the incoming currents might create a lateral stratification layer that limits the amount of mixing. Therefore, mixing layers are observed in very long distances downstream of the confluences (MacKay 1970). In contrast, studies such as Gaudet & Roy (1995) have shown that at certain hydrodynamic conditions as well as at specific flow depths of the stream, the pollution mixing through the confluence may intensify. Still, Lane *et al.* (2008) noticed that rapid mixing might occur downstream of a large river under proper flow and bathymetry conditions and suggested that these different confluence mixing rates depend on basin-scale hydrological responses, which may differ in upstream basins. Ramón *et al.* (2013) showed that the seasonal variability upstream of interconnected branches might also cause fluctuations in the water properties of interconnected streams and may affect the mixing mode and the resulting mixing layers. Parsons *et al.* (2007) showed that bedforms such as dunes could change the flow conditions in large rivers and prevent the formation of spiral flows expected at small-scale junctions. Biron *et al.* (2018) investigated the effect of ice cover at river junctions on mixing pollutants. Their research focused on a medium-width intersection in either the presence or absence of ice cover. Velocity profiles were then acquired along with the mixing layers. Finally, it has been observed that the presence of ice covers causes the formation of more significant velocity vectors in the middle of the channel, and the concentration and mixing of pollutants are also affected. Xiao *et al.* (2019) investigated the adsorption of phosphorus pollutants through confluences under the impact of three-dimensional flow patterns. The results showed that transverse and vertical velocities are two crucial and effective parameters in the P adsorption. Therefore, with increasing the values of these velocities, the degradation at the intersection decreases, and consequently, the lowest and highest P adsorption occurs in the maximum velocity and recirculation zones, respectively. Zhang *et al.* (2020) studied evolutions in river ecosystems due to contaminant mixing at river junctions. They performed several experiments on a wide, shallow-flowing river intersection and concluded that highly concentrated contaminated tributaries could alter the river confluence and downstream ecosystem. They also observed that the concentrations of pollutants change drastically over time. Lyubimova *et al.* (2020) investigated the effect of reducing the power of channel scaled secondary currents on the transverse dispersion of pollutants downstream of the confluence. They used Navier-Stokes's three-dimensional equations combined with the Reynolds stress turbulence model. They also used three types of cross-sections in their modeling and examined the featured secondary currents of each case. Yu *et al.* (2020) examined the accumulation of contaminated sediments through the river junctions due to special flow structures. They conducted experiments on a flume and examined variations in hydraulic conditions, contaminants, and morphodynamics. The observed results showed that the junction angle is the most critical factor influencing the release of contaminated sediments. van Rooijen *et al.* (2020) pointed out that changes in the density and temperature of the inflows through the river junction create three-dimensional flow structures. They used an idealized numerical model and observed that high and low-density flows move at low and upper parts, creating a shear layer between the two streams. Shin *et al.* (2021) studied the effect of recirculation zones of flow at river junctions on the level of pollution storage based on the angle of intersection. Their numerical studies focused on confluences with a grade of 30–90 degrees. The results showed that the length and width of the rotational zone increase with increasing the junction angle, and the rotational flow increases the vertical concentration gradient. Yuan *et al.* (2021) conducted two field studies to study the flow structure, suspended sediment concentrations, and the junction morphology on the Yangtze River. It was observed that in severe currents, dual rotating cores and, in low currents, only one rotating core is created. It was found that these rotating currents are the main factor in the sediment exchanging between different branches of a river confluence. Alizadeh & Fernandes (2021) investigated the effect of changing the discharge ratio and widths of different tributaries of a river intersection on the formed flow structures. It was concluded that changes in the input momentum of various branches significantly affect the position and types of figured flow structures.

As it can be concluded from the summary of previous studies, although many studies have been done on the erosion and sedimentation processes through the confluences, there is still insufficient information on the pollution mixing and distribution and the effective parameters. In this study, the effects of the injected pollutants concentration through branches of the river network and the water level difference between two branches on the mixing of contaminants were investigated. The connection angle of the tributary to the main channel of the river was considered to be 90 degrees. This study tried to discuss the observed hydrodynamic phenomena under the influence of velocity vectors and the distribution and mixing of the pollution entering from the sub-branch. Moreover, the spread of contamination concentration through the vertical flow direction was explored.

MATERIALS AND METHODS

Flow 3D is a powerful tool for computational fluid dynamics (CFD) calculation such that it can calculate many hydraulic and hydrodynamic parameters simultaneously. It is an accurate tool that helps researchers solve complex problems in a relatively fast time. This model works using basic fluid motion equations (Navier-Stokes and continuity equations). The continuity equation for the three-dimensional motion of the incompressible fluid follows Equation (1), and the Navier-Stokes equations in three dimensions follow Equation (2) (Ikinciogullari *et al.* 2022).

$$\frac{\partial u}{\partial x}+\frac{\partial v}{\partial y}+\frac{\partial w}{\partial z}=0 \tag{1}$$

$$\begin{aligned}
\rho\left(\bar{u}\frac{\partial \bar{u}}{\partial x}+\bar{v}\frac{\partial \bar{u}}{\partial y}+\bar{w}\frac{\partial \bar{u}}{\partial z}+\frac{\partial \bar{u}}{\partial t}\right) &= \rho X-\bar{u}\frac{\partial \bar{p}}{\partial x}+\mu\nabla^2\bar{u}+\frac{\partial}{\partial x}(-\rho\overline{u'u'})+\frac{\partial}{\partial y}(-\rho\overline{u'v'})+\frac{\partial}{\partial z}(-\rho\overline{u'w'})\\
\rho\left(\bar{u}\frac{\partial \bar{v}}{\partial x}+\bar{v}\frac{\partial \bar{v}}{\partial y}+\bar{w}\frac{\partial \bar{v}}{\partial z}+\frac{\partial \bar{v}}{\partial t}\right) &= \rho Y-\bar{u}\frac{\partial \bar{p}}{\partial y}+\mu\nabla^2\bar{v}+\frac{\partial}{\partial x}(-\rho\overline{v'u'})+\frac{\partial}{\partial y}(-\rho\overline{v'v'})+\frac{\partial}{\partial z}(-\rho\overline{v'w'})\\
\rho\left(\bar{u}\frac{\partial \bar{w}}{\partial x}+\bar{v}\frac{\partial \bar{w}}{\partial y}+\bar{w}\frac{\partial \bar{w}}{\partial z}+\frac{\partial \bar{w}}{\partial t}\right) &= \rho Z-\bar{u}\frac{\partial \bar{p}}{\partial z}+\mu\nabla^2\bar{w}+\frac{\partial}{\partial x}(-\rho\overline{w'u'})+\frac{\partial}{\partial y}(-\rho\overline{w'v'})+\frac{\partial}{\partial z}(-\rho\overline{w'w'})
\end{aligned} \tag{2}$$

In which ρ is mass density, $\bar{u}$ is the time averaged flow velocity in x direction, $\bar{v}$ is the time averaged flow velocity in y direction, $\bar{v}$ is the time averaged flow velocity in z direction, X, Y, and Z are specified Reynolds stress in the specified directions, $\bar{p}$ is the time averaged pressure, u' is the velocity fluctuation in x direction, v' is the velocity fluctuation in y direction, w' is the velocity fluctuation in the z direction.

For modeling the mixing process through the river confluences, a 3D model was created in AutoCAD. The mainstream length was assumed as 7 m, its width was 1 m, the length of the tributary was assumed as 1.8 m, and the width of the tributary was 1 m. Also, the model height of the junction was designed to be 1 m. Moreover, the junction angle of the tributary with the main channel was also assumed to be vertical. The schematic of the created model is drawn according to Figure 2. The total number of meshes considered for the main river mesh block and the sub-branch were 100,000 and 50,000, respectively. Additionally, a nested mesh block with 50,000 meshes was used to make the calculations more accurate through the confluence position (Figure 2(a)). The boundary condition is assumed to be constant pressure upstream of the main river and the connecting tributary. Moreover, a free outlet downstream of the main channel was assumed. Additionally, its boundary condition was also considered symmetrical due to the entry of boundary conditions from different aspects into the nested mesh (Figure 2(b)). P indicates a constant hydrostatic pressure at the inlet tributaries to the river confluence, and S means that the inlet and outlet flux to the boundary is zero.

RESULTS

It was observed that with increasing the water level difference between the pollutant carrier branch and the main channel, complete transverse mixing is done faster (Figure 3). However, for the case where there is no water level difference on both sides of the river intersection, the method of extracting the mixing curve was used to determine the length of the river where the transverse mixing is completed (Figure 4).

In addition, it can be said that due to the presence of rotational currents at the junction, the highest contaminant concentration was observed through the main branch of the stream at this point. This area is typically called recirculating zone. The most significant velocity vectors have been observed in this region, and the vertical and transverse flow rotation has been observed. It can be said that the secondary currents, created in this area, cause temporary trapping of some portion of the contaminant mass and increase its concentration (confirm the findings of Yu *et al.* 2020; Shin *et al.* 2021) (Figure 5(a)).

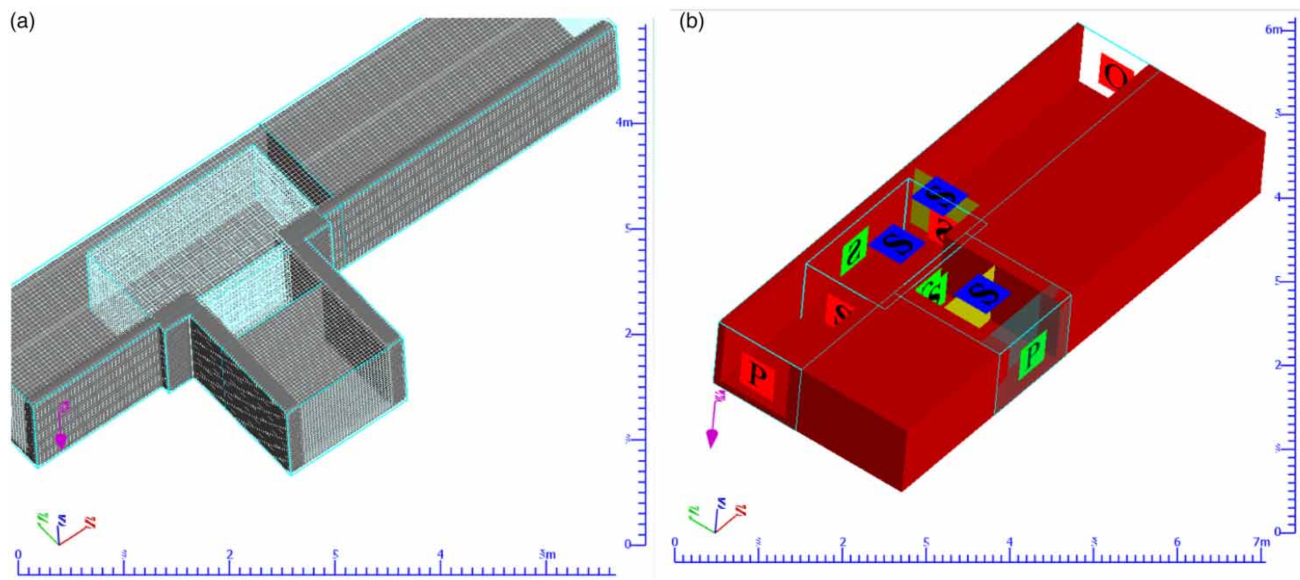

Figure 2 | (a) Schematic of a three-dimensional prepared model and its meshing for a river junction modeling; (b) considered boundary conditions for river junction model in Flow3D. P is illustrating constant hydrostatic pressure as entrance boundary condition, and S is symmetry boundary condition.

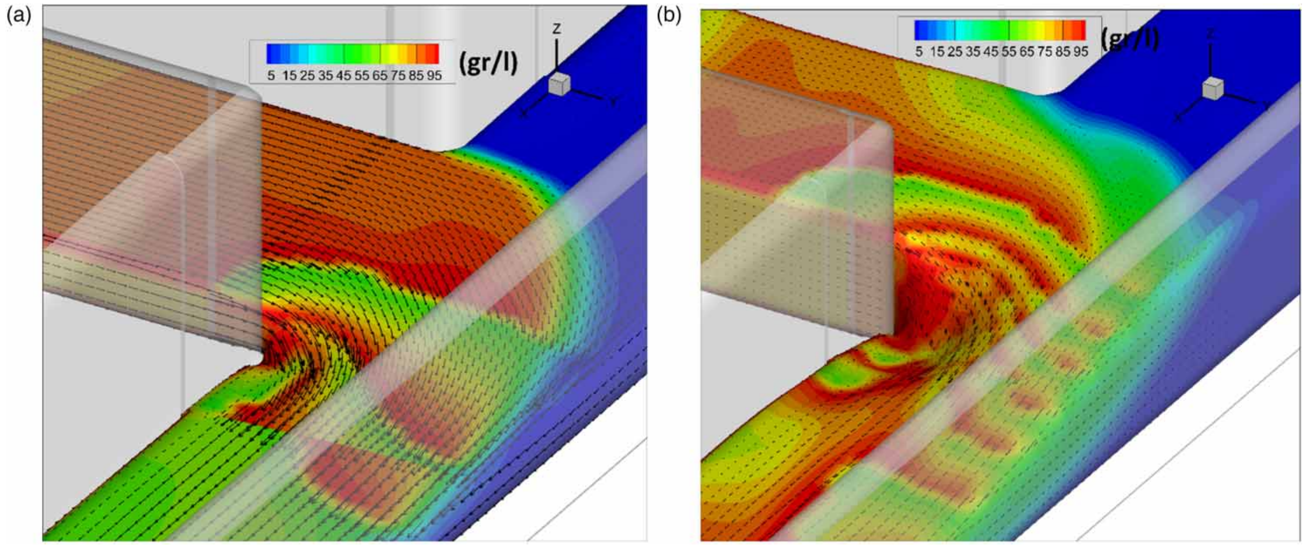

Figure 3 | Spread of pollution concentration (gr/L) (a). The water level in the sub-branch is 31 cm, and the water level in the main channel is 30 cm. (b) The water level in the sub-branch is 63 cm, and the water level in the main channel is 60 cm.

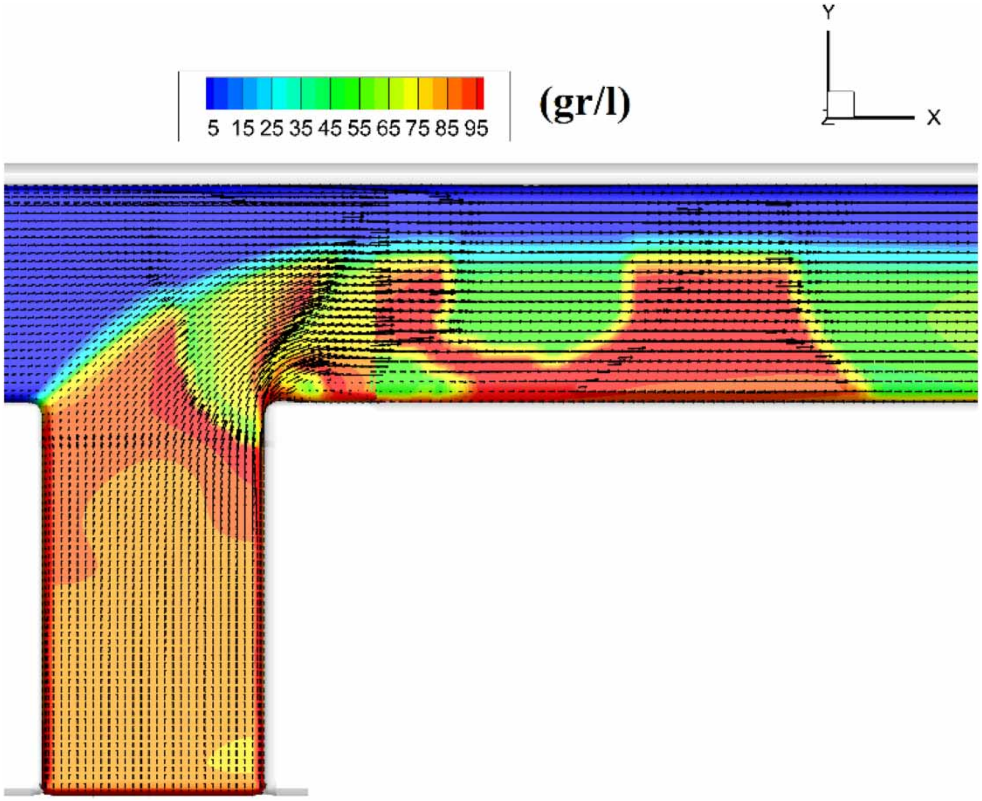

Figure 4 | Mixing layer formation and pollution spread (gr/L) when there is no difference in flow level on the sides of the junction.

The simulation results showed that the higher velocity gradient at the mixing boundary caused the shorter required length for complete transverse mixing. Outside this boundary, the flow deflection was observed upstream of the confluence. Also, in the deflection zone, there were weak secondary and rotational currents. It is noteworthy that the weakest velocity vectors were also observed in the stagnation region (Figure 5(b)).

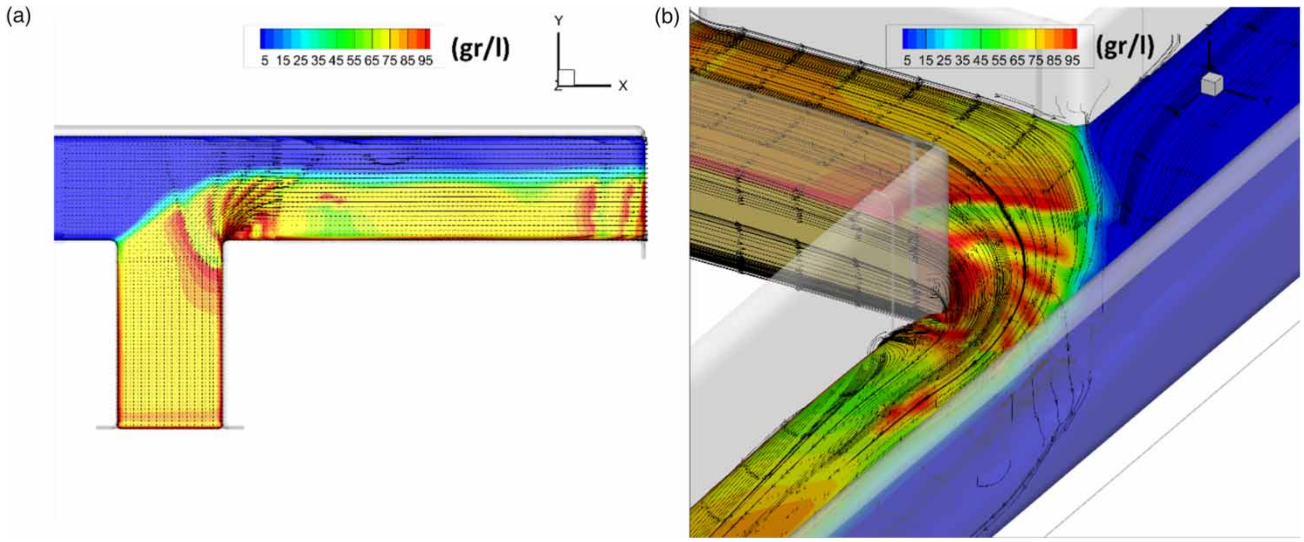

Figure 5 | (a) The size of the velocity vectors formed in the recirculation zone of the junction in comparison with the other parts of the confluence including contour type pollution concentration (gr/L); (b) formation of secondary currents and streamlines through the recirculation zone including contour type pollution concentration (gr/L).

Vertical study of pollutant distribution also showed that with approaching the rigid boundaries of the river junction as well as the free surface of the stream, a higher concentration is observed. Besides, it was found that the shallower the flow depth in the main channel and crossing branch of the river network, the lower the length required to complete the transverse mixing (Figure 6).

In the recirculation zone, the water level drop was also observed, and the orientation of the velocity vectors was downwards towards the channel bed. Totally, it can be concluded that the mentioned zone has a significant effect in the pollution spread through the main channel. Other identified hydrodynamic characteristics for this area include high shear velocity, high turbulence energy, and turbulence intensity, and also low longitudinal velocity, which is sometimes due to negative rotational currents. However, it can be said that the most important feature that causes contaminant dispersion at the river confluence is how the shear layer extends from the stagnation point towards the main channel of the river network

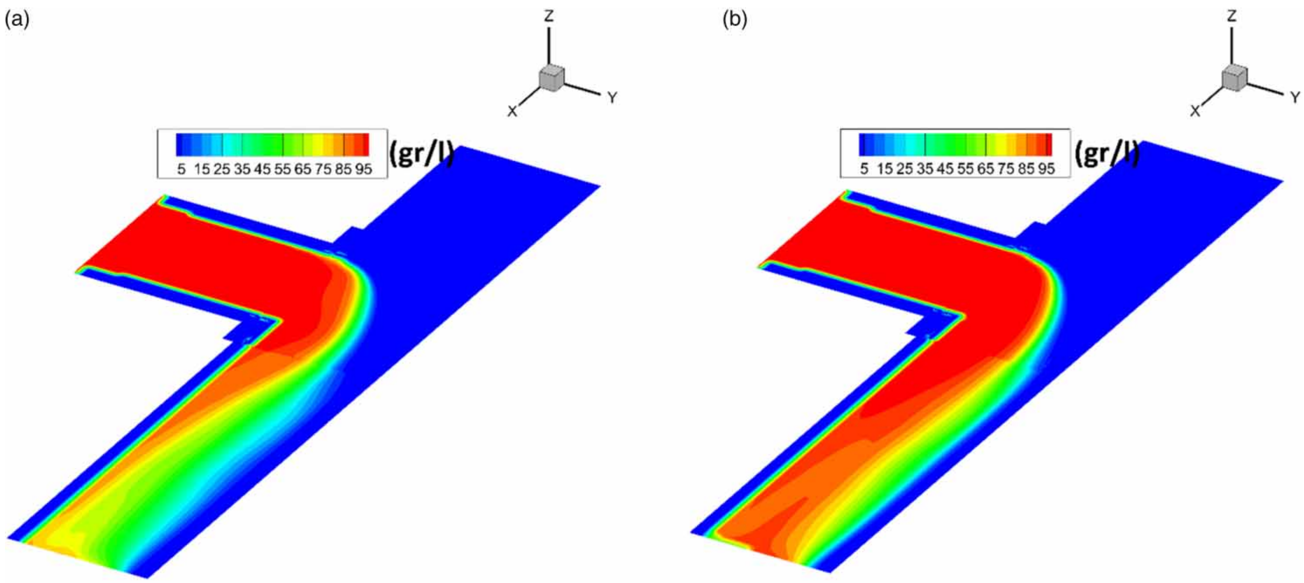

Figure 6 | (a) Contaminant concentration distribution (gr/L) at 13 cm distance from channel bed; (b) contaminant concentration distribution (gr/L) at 17 cm distance from the channel bed.

which confirms the findings of Liu *et al.* (2019). Many factors affect the position of this layer and the mass exchange rate of the pollutant in it. One of the most influential factors is the discharge and the water level difference on both sides of the junction. Due to the successive changes that occur in the river confluence morphology and bedforms, it may not be possible to comment definitively on the complete transverse mixing, and it is necessary to study the riverbed conditions, but the study of mixing in sedimentary beds is not aimed at the current research. It was observed that with a further increase of water level difference on both sides (an increase of water level height in the sub-branch), the contaminant concentration upstream of the confluence also increased. Moreover, the amount of pollution concentration was higher in the upstream and junction area rather than other zones, and it can be said that complete transverse mixing is observed over there. The spread of pollution concentration upstream of the junction is due to the rotational current creation through the flow surface and upstream of the junction. In other words, the results of the current study showed that unlike many parameters such as the connection angle of

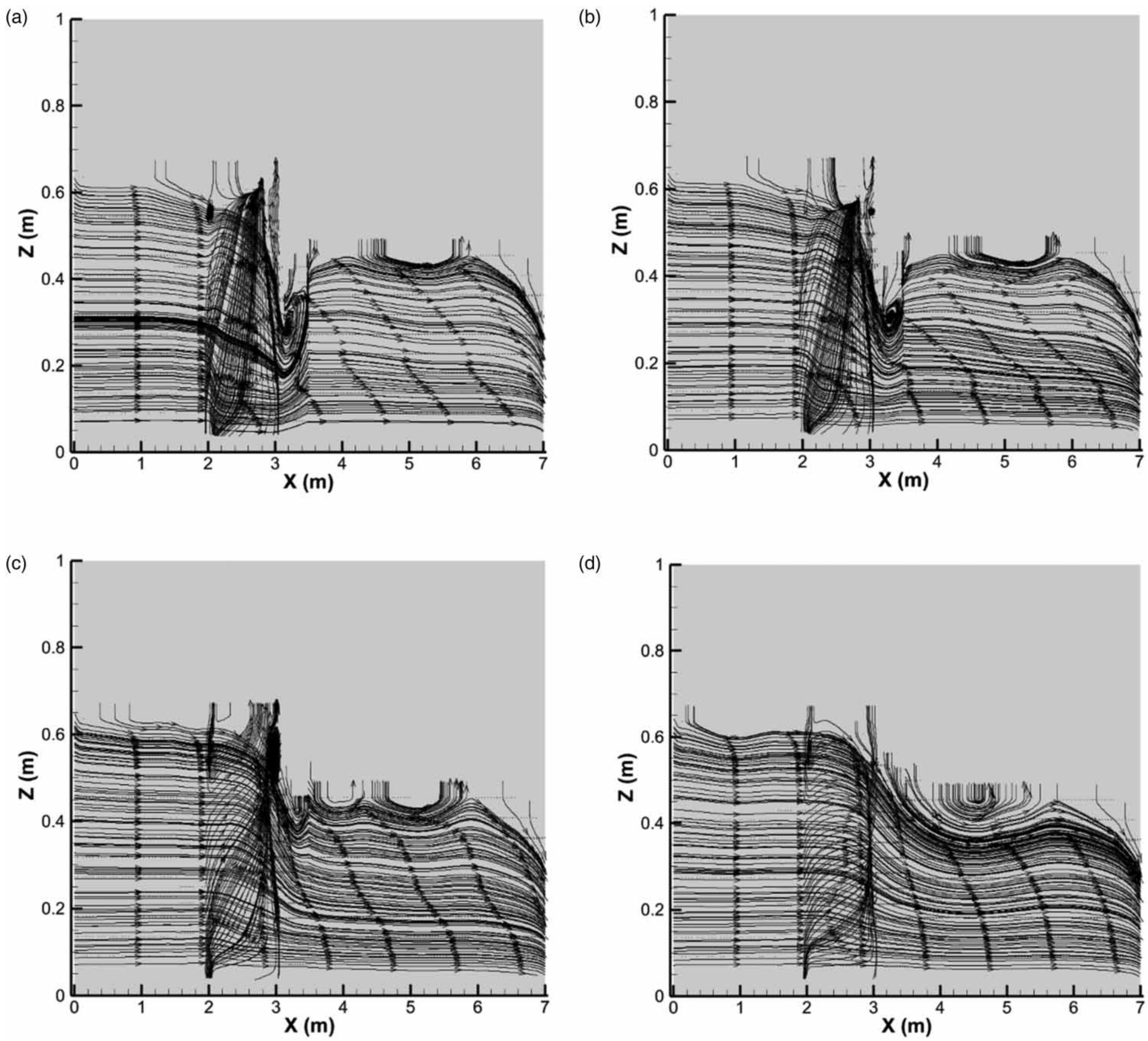

Figure 7 | (a) Streamline depiction through the longitudinal plane (x, z) at a distance of 180 cm (the beginning of the intersection of the branch to the main channel); (b) streamline depiction through the longitudinal plane (x, z) at a distance of 210 cm; (c) streamline depiction through the longitudinal plane (x, z) at a distance of 240 cm; and (d) streamline depiction through the longitudinal plane (x, z) at a distance of 270 cm (near to the side wall).

branches to each other, etc., water level difference is a more significant parameter in contaminant cross-sectional dispersion. Because during the floods, a large amount of sediment is usually washed and entered through the river's main channel, its occurrence is very likely. It was seen that with the dominance of the tributary flow to the main channel, an area with the maximum pollutant concentration was created on the other side of the riverbank (confirmed in the findings of Zhang *et al.* 2020). Besides, in contrast to the fact that the water level is the same on both sides of the confluence, the magnitude of pollutant concentration has increased on the river's left bank (the bank opposite the branch connection). The flow pattern and concentration spread were also changed at the stagnation point and recirculation zone. In general, two vortices and a diversion zone were observed in the river junction plan, which changed contaminant distribution upstream and downstream of the junction. In this case, the quantity of velocity vectors near the river bank has also increased. However, it can be said that the highest velocity values are related to the shear surfaces that extend from the sub-branch to the main channel. Examination of contamination contour lines also showed that the concentration of contaminants along these shear surfaces is higher than other sections and, in a way, it can be said that the formation of these surfaces has a significant role in transferring contaminant mass from the sub-branch to the main branch. It was also concluded that in order to reduce the contaminant effects through the river networks, the flow depth in the main channel should be greater than the sub-branches. Besides, increasing the flow velocity in the main branch also reduces the contaminant concentration and reduces the consequences of polluted flow diversion to the water supply systems.

The study of streamlines, drawn from velocity vectors, also showed that at the intersection of the branch to the main channel of the river, flow contraction is created, and the streamlines deviate towards the canal walls (Figure 7). It was also confirmed that the maximum values for velocity vectors along the shear surfaces, starting from the sub-branch, are valid for all cases. Comparing the values of velocity along the river banks, it was found that the velocity magnitude on the bank where the branch connects to the river is less than the next bank. Generally, it was seen that the direction of rotation of the vortices observed upstream and downstream of the river junction was clockwise, and the path of movement of the streamlines was from the depth to the flow surface (Figure 7). Examination of Fr number values showed that, in general, it could be concluded that its values after river junction are higher than upstream. However, if the flow blocking occurs downstream, it will affect the stream's overall condition. Furthermore, the vertical velocity values around the confluence zone revealed that the flow direction is from the surface towards flow depth, and the highest values of transverse velocity were observed in the recirculation zone (confirmed in the findings of Liu *et al.* 2019; Alizadeh & Fernandes 2021), causing flow deflection towards outer wall (Figure 8). The turbulent dissipation value in the recirculation region was higher than in other zones. The modeling results showed that a layer with the maximum turbulent kinetic energy starts from the recirculation region and develops downstream. Based on previous studies, it has been shown that the area between the recirculation zone and the flow

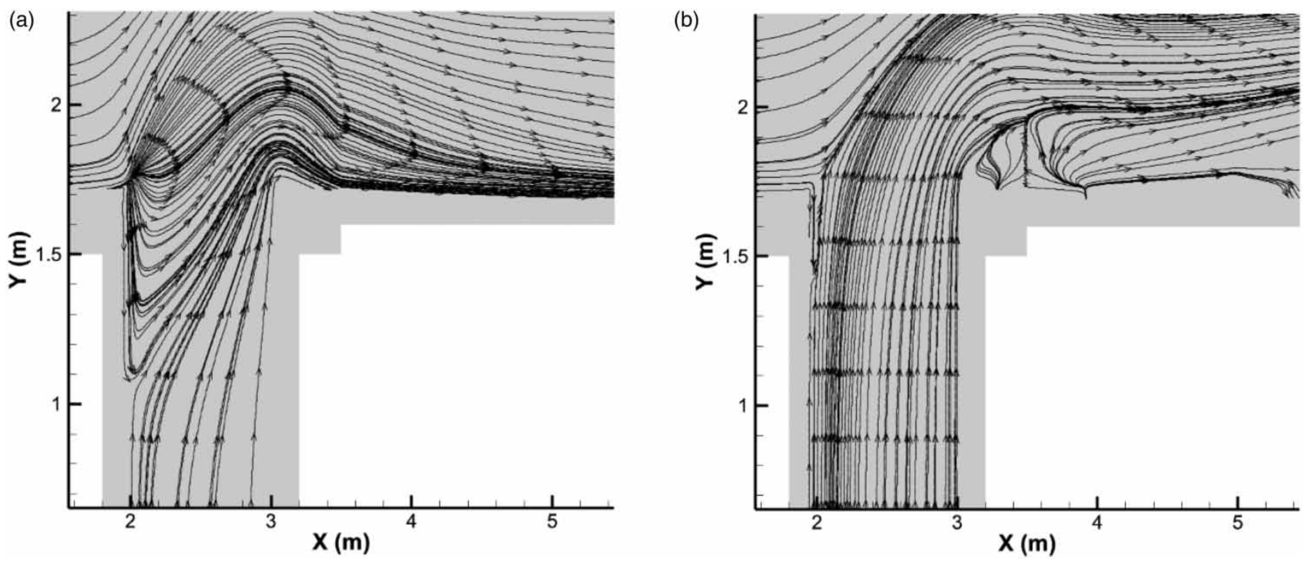

Figure 8 | (a) Streamline depiction at the height of 20 cm from the channel bed; (b) streamline depiction at the height of 40 cm from the channel bed.

deflection area is called the maximum velocity zone. During the current study, longitudinal velocity data averaged in-depth direction, confirmed their findings.

CONCLUSIONS

Due to the large volume of water supply for human consumption from the river network and the spread of pollutants entering the rivers from different places, it is essential to study the contaminant dispersion through the river junctions carefully. The numerical study conducted at the junction of 90 degrees showed that first, the water level difference is the most critical factor in the entry of pollutants from the tributaries to the main channel of rivers and to reduce the impact of the pollutants in the main rivers and subsequently in the human water supply system, water level regulation structures should be installed at the junctions. The previously observed flow patterns and flow zones at the junction were observed and confirmed in this study, and also the effect of each of them on the contaminant dispersion was discussed. It was concluded that the highest values of turbulence intensity, turbulence kinetic energy, velocity vectors, and contaminant concentration were observed through the flow recirculation zone. Furthermore, the vortices created in the recirculation zone and also their strength have an effective parameter in the temporary trapping of pollutants and increase of contaminant concentration. In addition, an increase in the pollution concentration upstream of the junction was observed only if flood flow occurs in the sub-branch and the water level in the sub-branch becomes higher than the main channel.

AVAILABILITY OF DATA AND MATERIAL

The datasets generated during and/or analyzed during the current study is available from the corresponding author on reasonable request.

CODE AVAILABILITY

Not applicable.

AUTHORS' CONTRIBUTIONS

Data analysis, conception or design of the work, simulation interpretation, and drafting the article.

ETHICS APPROVAL

Not applicable.

CONSENT TO PARTICIPATE

Not applicable.

CONSENT FOR PUBLICATION

Not applicable.

FUNDING

Not applicable.

DATA AVAILABILITY STATEMENT

All relevant data are included in the paper or its Supplementary Information.

CONFLICTS OF INTEREST STATEMENT

The authors declare there is no conflict.

REFERENCES

Alizadeh, L. & Fernandes, J. 2021 Turbulent flow structure in a confluence: influence of tributaries width and discharge ratios. *Water* **13** (4), 465.
Ashmore, P. E. 1991 How do gravel-bed rivers braid? *Canadian Journal of Earth Sciences* **28** (3), 326–341.

Ashmore, P. & Gardner, J. 2008 Unconfined confluences in braided rivers. In Rice, S. P., Roy, A. G. & Rhoads, B. L. (eds) *River Confluences, Tributaries and the Fluvial network* John Wiley & Sons, Chichester, UK, pp. 119–147.

Benda, L., Poff, N. L., Miller, D., Dunne, T., Reeves, G., Pess, G. & Pollock, M. 2004 The network dynamics hypothesis: how channel networks structure riverine habitats. *BioScience* **54** (5), 413–427.

Best, J. L. 1986 The morphology of river channel confluences. *Progress in Physical Geography* **10** (2), 157–174.

Best, J. L. 1987 *Flow Dynamics at River Channel Confluences: Implications for Sediment Transport and Bed Morphology*. SEPM Special Publication, Tulsa, OK, USA.

Best, J. L. 1988 Sediment transport and bed morphology at river channel confluences. *Sedimentology* **35** (3), 481–498.

Best, J. L. & Ashworth, P. J. 1997 Scour in large braided rivers and the recognition of sequence stratigraphic boundaries. *Nature* **387** (6630), 275–277.

Best, J. L. & Reid, I. 1984 Separation zone at open-channel junctions. *Journal of Hydraulic Engineering* **110** (11), 1588–1594.

Best, J. L. & Rhoads, B. L. 2008 Sediment transport, bed morphology and the sedimentology of river channel confluences. In Rice, S. P., Roy, A. G. & Rhoads, B. L. (eds) *River Confluences, Tributaries and the Fluvial Network* John Wiley & Son, Chichester, UK, pp. 45–72.

Best, J. L. & Roy, A. G. 1991 Mixing-layer distortion at the confluence of channels of different depth. *Nature* **350** (6317), 411–413.

Biron, P. M. & Lane, S. N. 2008 Modelling hydraulics and sediment transport at river confluences. In Rice, S. P., Roy, A. G. & Rhoads, B. L. (eds) *River Confluences, Tributaries and the Fluvial Network* John Wiley & Sons, Chichester, UK, pp. 17–43.

Biron, P., Best, J. L. & Roy, A. G. 1996a Effects of bed discordance on flow dynamics at open channel confluences. *Journal of Hydraulic Engineering* **122** (12), 676–682.

Biron, P., Roy, A. & Best, J. 1996b Turbulent flow structure at concordant and discordant open-channel confluences. *Experiments in Fluids* **21** (6), 437–446.

Biron, P. M., Ramamurthy, A. S. & Han, S. 2004 Three-dimensional numerical modeling of mixing at river confluences. *Journal of Hydraulic Engineering* **130** (3), 243–253.

Biron, P. M., Buffin-Bélanger, T. & Martel, N. 2018 Mixing processes at an ice-covered river confluence. In *E3S Web of Conferences*.

Boyer, C., Roy, A. G. & Best, J. L. 2006 Dynamics of a river channel confluence with discordant beds: flow turbulence, bed load sediment transport, and bed morphology. *Journal of Geophysical Research: Earth Surface* **111** (F4), 1–22.

Bridge, J. S. 1993 The interaction between channel geometry, water flow, sediment transport and deposition in braided rivers. *Geological Society, London, Special Publications* **75** (1), 13–71.

Chabokpour, J. & Samadi, A. 2020 Analytical solution of reactive hybrid cells in series (HCIS) model for pollution transport through the rivers. *Hydrological Sciences Journal* **65** (14), 2499–2507.

Chabokpour, J., Azamathulla, H. M., Azhdan, Y. & Ziaei, M. 2020a Study of pollution transport through the river confluences by derivation of an analytical model. *Water Science and Technology* **82** (10), 2062–2075.

Chabokpour, J., Chaplot, B., Dasineh, M., Ghaderi, A. & Azamathulla, H. M. 2020b Functioning of the multilinear lag-cascade flood routing model as a means of transporting pollutants in the river. *Water Supply* **20** (7), 2845–2857.

Ettema, R. 2008 Management of confluences. In Rice, S. P., Roy, A. G. & Rhoads, B. L. (eds) *River Confluences, Tributaries and the Fluvial Network* John Wiley & Sons, Chichester, UK, pp. 93–118.

Fielding, C. R. & Gupta, A. 2008 Sedimentology and stratigraphy of large river deposits: recognition in the ancient record, and distinction from 'incised valley fills'. In Gupta, A. (ed.) *Large Rivers: Geomorphology and Management* John Wiley & Sons, Chichester, UK, pp. 97–113.

Gaudet, J. M. & Roy, A. G. 1995 Effect of bed morphology on flow mixing length at river confluences. *Nature* **373** (6510), 138–139.

Ghostine, R., Vazquez, J., Terfous, A., Rivière, N., Ghenaim, A. & Mosé, R. 2013 A comparative study of 1D and 2D approaches for simulating flows at right angled dividing junctions. *Applied Mathematics and Computation* **219** (10), 5070–5082.

Holbrook, J. M. & Bhattacharya, J. P. 2012 Reappraisal of the sequence boundary in time and space: case and considerations for an SU (subaerial unconformity) that is not a sediment bypass surface, a time barrier, or an unconformity. *Earth-Science Reviews* **113** (3–4), 271–302.

Ikinciogullari, E., Emiroglu, M. E. & Aydin, M. C. 2022 Comparison of scour properties of classical and Trapezoidal Labyrinth Weirs. *Arabian Journal for Science and Engineering* **47**, 4023–4040.

Konsoer, K. M. & Rhoads, B. L. 2014 Spatial–temporal structure of mixing interface turbulence at two large river confluences. *Environmental Fluid Mechanics* **14** (5), 1043–1070.

Lane, S. N., Parsons, D. R., Best, J. L., Orfeo, O., Kostaschuk, R. & Hardy, R. J. 2008 Causes of rapid mixing at a junction of two large rivers: Río Paraná and Río Paraguay, Argentina. *Journal of Geophysical Research: Earth Surface* **113** (F2), 1–16.

Liu, X., Li, L., Hua, Z., Tu, Q., Yang, T. & Zhang, Y. 2019 Flow dynamics and contaminant transport in Y-shaped river channel confluences. *International Journal of Environmental Research and Public Health* **16** (4), 572.

Lyubimova, T. P., Lepikhin, A. P., Parshakova, Y. N., Kolchanov, V. Y., Gualtieri, C., Roux, B. & Lane, S. N. 2020 A numerical study of the influence of channel-scale secondary circulation on mixing processes downstream of river junctions. *Water* **12** (11), 2969.

Mackay, J. R. 1970 Lateral mixing of the Liard and Mackenzie rivers downstream from their confluence. *Canadian Journal of Earth Sciences* **7** (1), 111–124.

Mosley, M. P. 1976 An experimental study of channel confluences. *The Journal of Geology* **84** (5), 535–562.

Parsons, D. R., Best, J. L., Lane, S. N., Orfeo, O., Hardy, R. J. & Kostaschuk, R. 2007 Form roughness and the absence of secondary flow in a large confluence–diffluence, Rio Paraná, Argentina. *Earth Surface Processes and Landforms: The Journal of the British Geomorphological Research Group* **32** (1), 155–162.
Ramamurthy, A. S., Carballada, L. B. & Tran, D. M. 1988 Combining open channel flow at right angled junctions. *Journal of Hydraulic Engineering* **114** (12), 1449–1460.
Ramón, C. L., Hoyer, A. B., Armengol, J., Dolz, J. & Rueda, F. J. 2013 Mixing and circulation at the confluence of two rivers entering a meandering reservoir. *Water Resources Research* **49** (3), 1429–1445.
Rhoads, B. L. & Kenworthy, S. T. 1998 Time-averaged flow structure in the central region of a stream confluence. *Earth Surface Processes and Landforms: The Journal of the British Geomorphological Group* **23** (2), 171–191.
Rhoads, B. L. & Sukhodolov, A. N. 2001 Field investigation of three-dimensional flow structure at stream confluences: 1. Thermal mixing and time-averaged velocities. *Water Resources Research* **37** (9), 2393–2410.
Rhoads, B. L. & Sukhodolov, A. N. 2008 Lateral momentum flux and the spatial evolution of flow within a confluence mixing interface. *Water Resources Research* **44** (8), 1–17.
Richards, K. 1980 A note on changes in channel geometry at tributary junctions. *Water Resources Research* **16** (1), 241–244.
Riley, J. 2013 *The Fluvial Dynamics of Confluent Meander Bends*. University of Illinois at Urbana, Champaign, IL, USA.
Sambrook Smith, G. H., Ashworth, P. J., Best, J. L., Woodward, J. & Simpson, C. J. 2005 The morphology and facies of sandy braided rivers: some considerations of scale invariance. *Fluvial Sedimentology* **VII**, 145–158.
Schindfessel, L., Creëlle, S. & De Mulder, T. 2015 Flow patterns in an open channel confluence with increasingly dominant tributary inflow. *Water* **7** (9), 4724–4751.
Shit, P. K. & Maiti, R. 2013 Confluence dynamics in an ephemeral gully basin (A case study at Rangamati, Paschim Medinipur, West Bengal, India). *Research Journal of Applied Sciences, Engineering and Technology* **15** (5), 3895–3911.
Shin, J., Lee, S. & Park, I. 2021 Analysis of storage effects in the recirculation zone based on the junction angle of channel confluence. *Applied Sciences* **11** (24), 11607.
Song, C. G., Seo, I. W. & Do Kim, Y. 2012 Analysis of secondary current effect in the modeling of shallow flow in open channels. *Advances in Water Resources* **41**, 29–48.
Tang, H., Zhang, H. & Yuan, S. 2018 Hydrodynamics and contaminant transport on a degraded bed at a 90-degree channel confluence. *Environmental Fluid Mechanics* **18** (2), 443–463.
Van Rooijen, E., Mosselman, E., Sloff, K. & Uijttewaal, W. 2020 The effect of small density differences at river confluences. *Water* **12** (11), 3084.
Webber, N. B. & Greated, C. 1966 An investigation of flow behavior at the junction of rectangular channels. *Proceedings of the Institution of Civil Engineers* **34** (3), 321–334.
Xiao, Y., Xia, Y., Yuan, S. & Tang, H. 2019 Distribution of phosphorus in bed sediment at confluences responding to hydrodynamics. *Proceedings of the Institution of Civil Engineers-Water Management*, 149–162.
Yu, Q., Yuan, S. & Rennie, C. D. 2020 Experiments on the morphodynamics of open channel confluences: implications for the accumulation of contaminated sediments. *Journal of Geophysical Research: Earth Surface* **125** (9), 1–25. e2019JF005438.
Yuan, S., Tang, H., Xiao, Y., Qiu, X., Zhang, H. & Yu, D. 2016 Turbulent flow structure at a 90-degree open channel confluence: accounting for the distortion of the shear layer. *Journal of Hydro-Environment Research* **12**, 130–147.
Yuan, S., Tang, H., Xiao, Y., Chen, X., Xia, Y. & Jiang, Z. 2018 Spatial variability of phosphorus adsorption in surface sediment at channel confluences: field and laboratory experimental evidence. *Journal of Hydro-Environment Research* **18**, 25–36.
Yuan, S., Tang, H., Li, K., Xu, L., Xiao, Y., Gualtieri, C., Rennie, C. & Melville, B. 2021 Hydrodynamics, sediment transport and morphological features at the confluence between the Yangtze River and the Poyang Lake. *Water Resources Research* **57** (3), 1–21. e2020WR028284.
Zhang, T., Feng, M., Chen, K. & Cai, Y. 2020 Spatiotemporal distributions and mixing dynamics of characteristic contaminants at a large asymmetric confluence in northern China. *Journal of Hydrology* **591**, 125583.

First received 20 December 2021; accepted in revised form 27 May 2022. Available online 16 June 2022